# Formation of an Ordered Ice Layer on a Thin Silica Film

**S. Kaya, J. Weissenrieder, D. Stacchiola, S. Shaikhutdinov,* and H.-J. Freund**

*Fritz-Haber-Institut der Max-Planck-Gesellschaft, Faradayweg 4-6, 14195 Berlin, Germany*

*Received: July 7, 2006; In Final Form: October 10, 2006*

Adsorption of water on a thin silica film grown on a Mo(112) single crystal was studied by temperature-programmed desorption, infrared reflection absorption spectroscopy, and photoelectron spectroscopy using synchrotron radiation. Water does not dissociate on the defect-free oxygen-terminated silica surface. In contrast to adsorption at 100 K, where water follows a zero-order desorption kinetics, water adsorbed at 140 K exhibits a pseudo-first-order kinetics and induces a strong blue shift of the silica phonon. Even larger spectral changes were observed for $D_2O$ adsorption. The results were rationalized in terms of the formation of an amorphous solid water film at 100 K and a crystalline ice monolayer film at 140−150 K. This film is well-ordered as revealed by low-energy electron diffraction showing a $c(2 \times 2)$ superstructure with respect to the silica substrate.

## 1. Introduction

Water plays an important role in many technical fields such as material science, atmospheric chemistry, and catalysis. Surface science studies on water adsorption on solid surfaces have been reviewed by Thiel and Madey[1] and recently by Henderson.[2] In spite of a vast amount of studies reported, the adsorption of water is still debated, even for the systems extensively investigated for years like, for instance, Pt(111), Pd(111), and Ru(0001).[3−10] It has been shown that water monomers are formed on metal surfaces at low coverage and very low temperatures (typically <40 K), which cluster into amorphous solid water (ASW) on heating above 60 K due to enhanced water diffusion on the surface.[11,12] Upon further heating to or dosing at 125−135 K, crystalline ice (CI) forms. Based on the diffraction studies, it has been suggested that the multilayer CI films exhibit cubic ice structure ($I_c$) which is in fact very similar to the structure of the hexagonal ice ($I_h$).[13−15]

In the bilayer model of ice on metal surfaces, first proposed by Kretzschmar et al.[16] and Doering and Madey,[13] the first layer consists of nearly in-plane water molecules bound to the metal surface via an oxygen lone pair, while water molecules in the second layer are in-plane with a surface normal. Only one H atom from the top-laying molecules is involved in the formation of a H-bond network to the water molecules in the first layer; another H atom pointed away from the surface (referred to as "H-up" model). However, recent theoretical results[17] suggest that this OH bond points to the Pt surface ("H-down" model), leaving no dangling OH bonds protruding into the vacuum, thus explaining the nonwetting behavior of the next ice agglomerates on top of the "hydrophobic" water bilayer as experimentally observed by Kimmel et al.[18] The formation of an epitaxial CI film may lead to long-range ordered structures observed by low-energy electron diffraction (LEED) like, for example, $(\sqrt{39} \times \sqrt{39})$ R16.1° on Pt(111)[3] and $(\sqrt{3} \times \sqrt{3})$ R30° on Ru(0001).[13,14]

With use of scanning tunneling microscopy operating at low temperatures, cyclic water hexamers have been observed on Pt(111), Cu(111), and Ag(111) surfaces.[19−21] Based on density functional theory calculations, these hexamers were explained as rings of nearly flat-lying water molecules which are considered as building units for the two-dimensional growth of ice on Pd(111).[22] Very recently, Yamada et al. reported on self-assembly of water molecules into one-dimensional zigzag chains on the Cu(110) surface at low coverage due to the anisotropy of the substrate.[23]

Formation of the CI films on oxide surfaces has been studied to a lesser extent.[24−27] To date, MgO(100) seems to be the only surface for which ordered water overlayers have been observed, although different structures were reported. Heidberg et al.[28] found a $c(4 \times 2)$ structure by low-energy electron diffraction (LEED), while Goodman and co-worker[29] using MgO(100) films grown on Mo(100) reported on $p(3 \times 2)$ LEED pattern. Recent studies by Ferry et al. show that there is a delicate balance between wetting and clustering on MgO(100) which may strongly depend on the experimental conditions.[30,31] In addition, several theoretical studies suggest that a mixed (water + hydroxyl) layer is thermodynamically more stable than water bilayer, which implies water dissociation on MgO(100); however, this issue remains controversial.[32,33]

It is expected that oxygen-terminated defect-free oxide surfaces do not dissociate water. Indeed, Tzvetkov et al. found no evidence for water dissociation on thin alumina film grown on NiAl(110).[34] Based on work function measurements, photoelectron spectroscopy using synchrotron radiation (PES), and ultraviolet photoelectron spectroscopy (UPS), the authors suggested that isolated water molecules start to cluster above 0.5 Langmuir (1 L = $10^{-6}$ Torr s) exposure at 100 K, finally forming three-dimensional (3D) ice multilayers.

Also, Weiss and co-workers observed only molecular water adsorption on oxygen-terminated FeO(111) films grown on Pt(111).[35] Based on temperature-programmed desorption (TPD) and UPS results, they have proposed that water first adsorbs at 100 K as monomers in upright geometry with the oxygen atom pointed toward the Fe ions underneath the top O-layer. At increasing water coverage, formation of the CI film in a "H-up" geometry has been suggested. In contrast, Kay and co-workers[36] have found no evidence for isolated water monomers even at 30 K using TPD of $N_2$ and infrared reflection absorption spectroscopy (IRAS). The authors suggested formation of ordered ice islands wetting the FeO(111) surface at 135

* Corresponding author. E-mail: shaikhutdinov@fhi-berlin.mpg.de.

10.1021/jp064283e CCC: $37.00 
Published on Web 12/06/2006

K. However, no long-range water ordering was observed by LEED in both studies. It should be mentioned however that these two groups have presented quite different TPD spectra of water at submonolayer coverage, which may be related to the morphology and defect structure of the films studied. Indeed, our own STM studies showed that the FeO(111) films may possess small holes and/or exhibit ill-defined particles whose presence cannot be excluded on the basis of conventional LEED measurements.[37] Therefore, it is important that the surface morphology of the oxide films be controlled in these experiments to interpret adsorption results.

It should also be mentioned that a long-term interest of the research groups in formation of ice films is partially driven by attempts to grow a thin, well-ordered ice film which allows one to employ various surface-sensitive techniques for studying chemical reactions on ice. It is obvious that the epitaxial growth of ice on any substrate is favored by a small lattice mismatch between them. The O−O distance in the $I_h$ phase is 2.75 Å (2.61 Å when projected onto the (0001) plane), which is much shorter than 3−3.1 Å for the close-packed FeO(111) as well as alumina film surfaces mentioned above. However, a well-ordered silica film grown on a Mo(112) single crystal[38,39] exhibits a slightly distorted hexagonal lattice with an O−O distance in the top layer equal to 2.73 Å and therefore can be considered as a good substrate for the epitaxial growth of ice. This silica film consists of a two-dimensional (2D) network of corner-sharing [$SiO_4$] tetrahedra, with one of four oxygen in each tetrahedra binding to the Mo substrate. The interaction of water with differently prepared silica films was previously studied by Wendt et al., who have proposed that water forms 3D clusters at 90 K even at low coverages and does not dissociate on the surface upon heating.[40]

In this paper, we present experimental results on water adsorption on silica/Mo(112) using TPD, IRAS, and PES, which show that, under certain conditions, the ice layer is in a good epitaxial relationship with the silica surface and forms a long-range ordered structure as observed by LEED.

## 2. Experimental Section

The experiments were performed in two different ultrahigh vacuum (UHV) chambers (base pressure below $2 \times 10^{-10}$ mbar). One chamber was equipped with an STM (Omicron), UPS/XPS (Scienta 200), an IR-spectrometer (Bruker i66/vs) and standard facilities for sample preparation. TPD studies were carried out in another UHV chamber equipped with a differentially pumped mass spectrometer (QMS, Fision) and AES/LEED (Omicron).

The ultrathin silica films were grown as follows. The clean Mo(112) surface was exposed to $5 \times 10^{-8}$ mbar of oxygen at 900 K for 5 min, followed by ca. 1.2 monolayer (ML) of Si vapor deposition in the same oxygen pressure and temperature. The sample was then annealed in vacuum to 1250 K for 5 min. The quality of the films was checked by STM, which showed the atomically flat surface without any silica particles (typically observed by annealing at lower temperatures). The IR spectra were measured with p-polarized light at 84° grazing angle of incidence (resolution $\sim$ 2 $cm^{-1}$). Water ($H_2O$ and $D_2O$) was exposed to the surface using a directional gas doser inside the IRAS cell.

The recipe for the preparation of the silica film in the TPD chamber was identical to that used for the IRAS studies. Water was adsorbed via a directional gas doser, which was calibrated with water adsorption on Pt(111), where the formation of water bilayer can be discriminated by TPD.[18,41] Henceforth, bilayer water equivalent (BLE) will be used as a measure of water coverage. For TPD experiments, the sample was placed $\sim$0.5 mm from the nozzle of the QMS shield to avoid desorption signals from the heating wires. The temperature and linear heating rate were precisely controlled by the feedback system (Schlichting Phys. Instrum.). The temperature was measured by a type C thermocouple spot welded to the edge of the Mo(112) crystal.

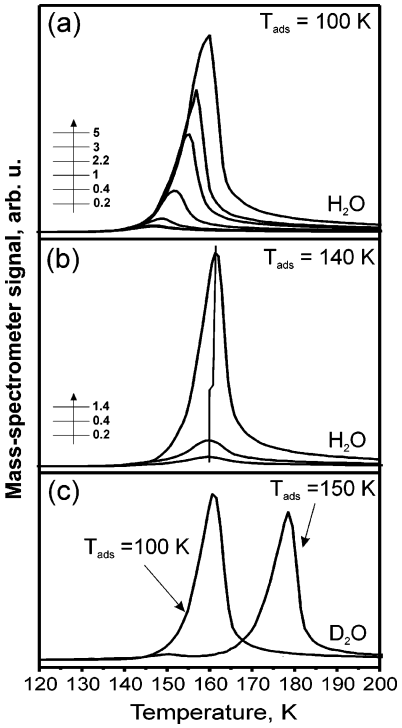


**Figure 1.** TPD spectra of $H_2O$ adsorbed on the silica film at 100 K (a) and 140 K (b) at different coverages as indicated. (c) TPD spectra of $D_2O$ adsorbed at 100 and 150 K to the same water coverage ($\sim$1 BLE). Heating rate was 3 K/s for each spectrum.

The PES measurements were performed using the synchrotron facilities at BESSY II in Berlin (beamline UE52-PGM1). The spectra were recorded with a Scienta R4000 analyzer at normal electron emission. The O 1s level spectra were measured at photon energies of 630 eV (spectral resolution below 200 meV). The binding energies were calibrated with respect to the Fermi edge.

## 3. Results

**3.1. Temperature-Programmed Desorption.** Figure 1a shows a family of TPD spectra as a function of $H_2O$ exposure at 100 K. These spectra show a zero-order desorption kinetics of "multilayer" water as was observed on many solid surfaces.[34,42−45] The same kinetics is observed for $D_2O$ adsorption, with the desorption temperature shifting by $\sim$10 K to higher temperatures as compared to $H_2O$ at a given coverage. The analysis of the leading edge of these TPD spectra revealed desorption energies of 45 and 51.5 kJ/mol for $H_2O$ and $D_2O$, respectively, which are consistent with heats of sublimation reported in the literature.[1,46,47] No features indicating transition from monolayer to multilayer desorption have been observed in the TPD spectra (as is on Pt(111), for example[18]), which implies formation of an overlayer where the interaction with the substrate is weaker than that between the water molecules.

However, water dosing at 140 K (i.e., the edge of $H_2O$ desorption) results in desorption with a pseudo-first-order kinetics as shown in Figure 1b. The top spectrum in Figure 1b

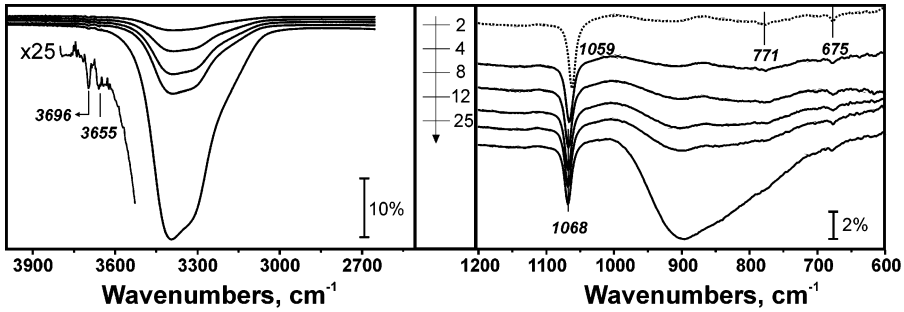


**Figure 2.** IRAS spectra of $H_2O$ adsorbed on the silica film at 100 K at increasing coverage as indicated.

corresponds to the highest coverage (~1.4 BLE) reached under these conditions (which in fact critically depends on the balance between the sample cooling rate and the water pumping speed since water starts to desorb at this temperature but may re-adsorb while cooling). Comparison of two sets of spectra showed that $H_2O$ adsorbed at 140 K desorbs at temperatures ~7 K higher than water exposed at 100 K up to the same coverage. Even a larger difference ($\Delta T \sim 18$ K) is observed for $D_2O$ (see Figure 1c), when adsorption at 100 and 150 K (the edge of $D_2O$ desorption) is compared. The multilayer films grown by water exposure at 135 K (145 K for $D_2O$) were found to desorb in a single peak too, and at temperatures ~5 K higher than the films grown at 100 K at a given water coverage (not shown here).

These findings indicate that two different structures are formed by adsorption at low and high temperatures (100 and 140 (150) K, respectively). Figure 1c clearly shows that the desorption signal from the "high-temperature" structure cannot comprise the high-temperature tail of the TPD traces of water adsorbed at 100 K. Note, also, that the TPD spectra did not reveal any feature for heating rates of 0.2−3 K/s, which could be associated with the structural transformations upon heating in a definitive manner. Therefore, we conclude that the surface restructuring proceeds slower than the time scale of the TPD experiment (typically 10−20 s).

Interestingly, any attempts to resolve two desorption states in TPD spectra by additional adsorption at 100 K on the sample pre-exposed to $H_2O$ at 140 K were unsuccessful as it always resulted in the same TPD spectra as for water exposed only at 100 K.

**3.2. Infrared Reflection Absorption Spectroscopy.** Figure 2 shows IRAS spectra of the silica film as a function of water exposure at 100 K. Here, we have to recall the vibrational frequencies of molecular water as follows:[48−51] Hydrogen-bonded O−H stretches at 3000−3600 $cm^{-1}$, bending mode at 1500−1650 $cm^{-1}$, and librations at 700−1000 $cm^{-1}$. In addition, a weak signal at around 3700 $cm^{-1}$ is typically assigned to the stretch of dangling O−H bonds having no hydrogen bond to water molecules on the surface of 3D clusters.[50,52,53] For dissociative water adsorption on oxides, the signals from isolated OH species adsorbed on the oxide surface are typically below 3700 $cm^{-1}$, for example, 3620 $cm^{-1}$ for $Cr_2O_3$[54] and 3660 $cm^{-1}$ for $Fe_3O_4$.[55]

The OH stretching region of the IRAS spectra, presented in the left diagram of Figure 2, with a broad band centered at ~3400 $cm^{-1}$, is typical for the ASW phase.[36] In addition, two weak signals at 3696 and 3655 $cm^{-1}$ (2727 and 2700 $cm^{-1}$ in the case of $D_2O$ adsorption) can be detected. The feature at 3696 (2727) $cm^{-1}$ is assigned straightforwardly to the dangling OH (OD) bonds on the ASW surface,[50,52,53] while the signal at 3655 (2700) $cm^{-1}$ can be attributed to isolated OH (OD) species formed on the defect sites of the silica film. This signal is very weak since the silica films used in these experiments showed a low density of defects as evidenced by STM images of the films prior to water adsorption. Therefore, the IRAS results indicate that water does not dissociate on the oxygen-terminated silica film.

The clean silica film is characterized by a sharp phonon signal at 1059 $cm^{-1}$, assigned to the Si−O−Mo stretching vibrations, and also weak bands at 771 and 675 $cm^{-1}$, assigned to the coupled stretching and bending modes.[38,39] As shown in the right diagram of Figure 2, water adsorption gradually shifts the main peak by ~9 $cm^{-1}$ toward higher frequencies without significant loss of the intensity, which then stays nearly constant, although the water coverage increases as evidenced by continuous growth of the broad bands centered at ~3400 and ~900 $cm^{-1}$. The same ~9 $cm^{-1}$ shift has been observed in similar experiments with $D_2O$.

On slow heating of the sample used in Figure 2, the phonon absorption peak at 1068 $cm^{-1}$ splits into two peaks: one peak at 1059 $cm^{-1}$ as in the original silica film and a high-frequency peak as shown in Figure 3. This splitting appears simultaneously with the spectral changes in the OH stretching region (left panel), which are characteristic of ice crystallization.[25,56] Upon further heating, the CI film sublimates (the OH-band intensity scales down) and the blue-shifted peak gradually vanishes while the peak at 1059 $cm^{-1}$ from the bare silica gains the intensity. The high-frequency peak continuously shifts up to 1082 $cm^{-1}$ until complete desorption of the film. The blue-shifted peak emerges from the onset if the water is dosed at temperatures above water crystallization temperature (not shown here), thus indicating that this crystalline structure is thermodynamically stable.

Finally, in contrast to adsorption at 100 K, where the same ~9 $cm^{-1}$ shift of the silica phonon was observed both for $H_2O$ and for $D_2O$, the IRAS spectra for the CI films revealed isotopic effect such that the phonon splitting, observed upon heating of the $D_2O$ film, is by 5−10 $cm^{-1}$ larger than that for $H_2O$. The experiments with the silica film prepared with $^{36}O_2$ isotope showed essentially the same behavior, which confirms that all the effects observed above originate from the water/silica interaction.

**3.3. Photoelectron Spectroscopy.** Figure 4 shows the O 1s PES spectra of the silica film exposed to water at 90 K. Two O species at 532.5 and 531.3 eV observed on the clean film have been previously assigned to the O atoms in the topmost (O−Si−O) and interface (Si−O−Mo) layers, respectively.[38] Note that to minimize the photon-induced changes in the water overlayer, we slowly moved the sample while recording the consecutive spectra at the lowest acquisition time (typically 10 s each) and photon dosage. Adsorption of 6 L of water results in a signal centered at 534.3 eV, which can be attributed to the intact water molecules.[34] Upon slow heating, this signal gradually attenuates, finally resulting in the spectrum of the clean silica surface. Due to a relatively broad spectral feature of water, it is difficult to follow a crystallization process as observed by

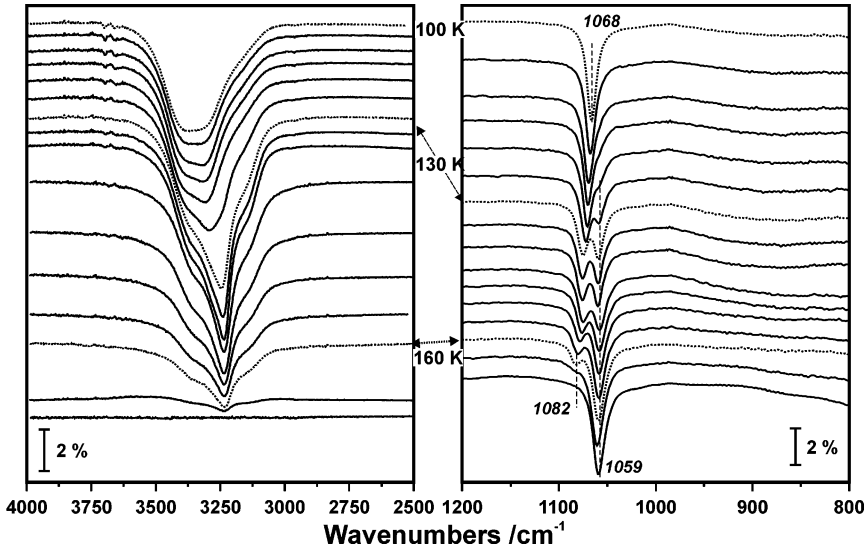


**Figure 3.** IRAS spectra of 6 BLE of $H_2O$ adsorbed on the silica film at 100 K and slowly heated up to complete desorption of the ice film. Three spectra at indicated temperatures are presented as dotted lines.

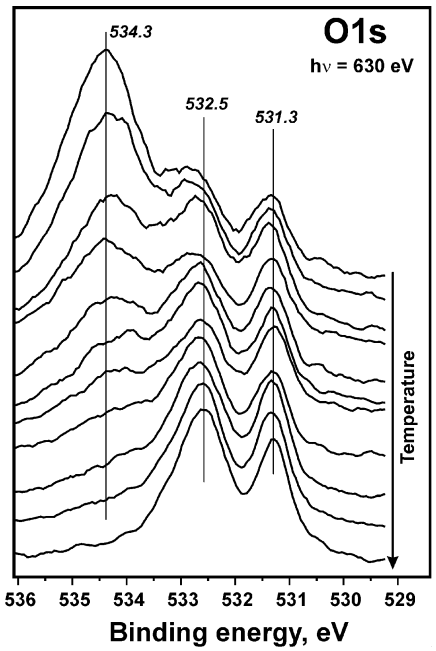


**Figure 4.** Consecutive PE spectra of the silica film, exposed to 6 L of water at 100 K, on slow heating to 170 K ($\Delta T \sim 5$ K per spectrum). The states at 532.5 and 531.3 eV are assigned to the surface and interfacial O species in the silica film.[38] The spectra were recorded at low integrated photon dosage to prevent any photon-induced damaging effects. The spectra are offset for clarity.

IRAS. However, no hydroxyl species (expected at ~533.5 eV) were detected upon heating to 200 K, which is consistent with nondissociative adsorption of water. Note also that the IRAS study of the samples before and after XPS and LEED experiments revealed no electron-induced dissociation of water.

## 4. Discussions

The combined TPD, IRAS, and PES study shows that water does not dissociate on the silica film, in agreement with previous observations by Wendt et al.[40] The TPD results clearly show that two energetically different structures are formed by adsorption at 100 and 140 K, which follow different desoprtion kinetics. Based on the IRAS data, showing characteristic changes in the OH stretching region, these structures can be assigned to the amorphous (ASW) and crystalline (CI) films, respectively. The "high-temperature" structure is thermodynamically stable since it can be formed either by heating of the ASW film to or by water exposure directly at 140 K. However, the structural transformations are quite slow (likely, in $10^2$−seconds scale) and cannot be discriminated by TPD at the heating rates studied (0.2−3 K/s).

The formation of the CI film significantly modifies the vibrational properties of the silica film, resulting in a remarkable blue shift of the Si−O−Mo stretching frequency. The experiments with the silica film prepared with $^{36}O_2$ confirm that this effect originates from the water/silica interface. In addition, both TPD and IRAS studies have revealed isotopic effects such that the spectral changes between the ASW and CI films are larger for $D_2O$ than for $H_2O$. Interestingly, the blue shifts in IRAS spectra seem to correlate with the temperature shifts in TPD spectra (e.g., ~7 K and 17 $cm^{-1}$ for $H_2O$ vs 18 K and 26 $cm^{-1}$ for $D_2O$ at the same water coverage).

In principle, there are several factors which may influence phonon spectra of thin oxide films in the presence of deposits and adsorbates as systematically studied by Frank et al. on alumina.[57] However, our previous studies showed that metal and oxide particles, deposited on thin alumina and silica films, always led to a red shift and simultaneous broadening of the oxide phonon at increasing coverage.[58,59] Any sorts of phonon coupling must be excluded as the vibration frequencies in water and silica film are energetically well-separated. On the other hand, water is a polar molecule and has a large dipole moment; therefore, it seems plausible that the effect observed here for water is caused by polarization of the water/silica interface, which influences the Si−O−Mo stretching vibration.

A gradual shift of the silica phonon peak observed upon water adsorption at 100 K (~9 $cm^{-1}$, at saturation) is likely caused by the ASW film where the water molecules are randomly oriented with respect to the silica surface underneath. This implies that the ASW film does not wet the substrate. Most likely, the ASW film uniformly covers the surface via water clusters ("particles") and their agglomerates, ultimately forming a thin "microporous" film at high water exposures. On heating, the crystallization may occur within the existing morphology of the ASW film (topochemical transformations) and involve only local bonds rearrangement or it may accompany the overall mass transport due to increasing surface diffusivity of the water

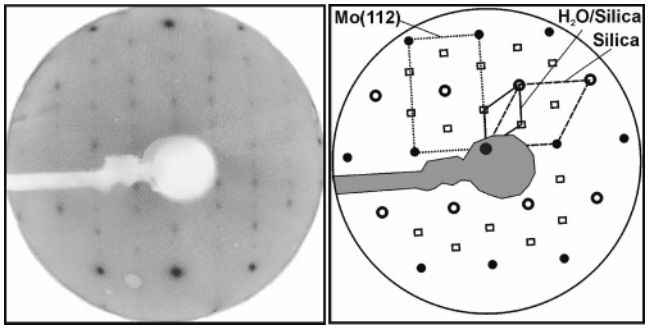


**Figure 5.** LEED pattern (negative contrast) and its schematic presentation developed at around 145 K during heating of the 4 BLE film, initially adsorbed at 100 K, on the silica film detected upon slow heating (0.2 K/s) of the ASW film. The unit cells of Mo(112)-(1 × 1), silica film ($c$(2 × 2)-Mo), and the ice layer ($c$(6 × 2)-Mo) are indicated. (Note that the patterns could also show additional weak spots assigned to the (3 × 2) structure).

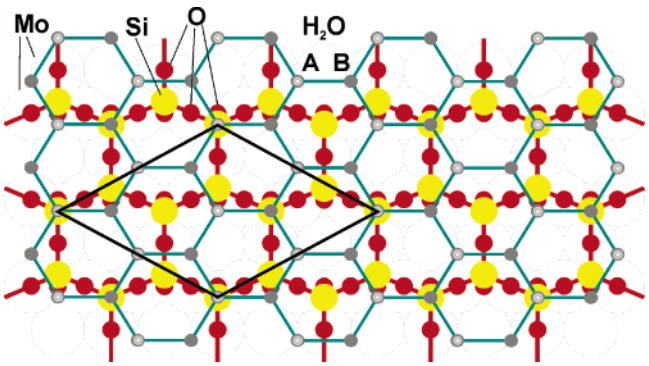


**Figure 6.** Structural model of the ice layer formed on the silica film, which exhibits a $c$(6 × 2)-Mo(112) or $c$(2 × 2)-$SiO_2$ superstructure as indicated by a rhomb. A and B indicate differently oriented water molecules within a bilayer model.

molecules. Therefore, observation of the phonon peak at 1059 $cm^{-1}$ from the bare silica upon the crystallization may be due to a restructuring ("disproportionation") of the water/silica interface. This crystallization causes a much stronger shift of the silica phonon, which indicates the formation of the *ordered* structure of the crystalline ice on the silica substrate.

To verify this hypothesis, we have employed LEED in combination with TPD. Diffraction patterns from the sample exposed to water at 140 K indeed showed new diffraction spots. However, the intensity of the water-induced spots depended on the preparation conditions due to water re-adsorption from the vacuum background during cooling. To find conditions for the best ordering and estimate the water coverage, at which the ordered structure appears, we monitored the LEED pattern while heating the water/silica samples at different heating rates. The typical pattern observed this way is shown in Figure 5, which was found to exist for a short time at temperatures very close to the maximum desorption temperature as simultaneously monitored by a mass spectrometer. This suggests that the ordered film is formed at low, probably submonolayer, coverage and may explain why observation of the ordered structure critically depends on the temperature. The analysis of the LEED patterns showed that the CI layer basically exhibits a $c$(6 × 2) structure with respect to Mo(112)-(1 × 1) which may coexist with a (3 × 2) structure. The latter exhibits relatively weak spots depending on beam energy.

Based on these observations, we propose a model depicted in Figure 6. Since the CI films strongly affect the Si−O−Mo stretching (see Figure 3), it is reasonable to assume that the water molecules are bonded to silica through the O atoms sitting above the $Si^{4+}$ cations. Previously, Joseph et al.[35] on the FeO-(111) film and Tzvetkov et al.[34] on the alumina film also suggested that water adsorbs through oxygen pointing to the metal cations ($Fe^{2+}$ and $Al^{3+}$, respectively) located in the hollow sites underneath the surface O-layer. As a starting point, we adopt a bilayer model of the first ice layer (which henceforth will be referred to as "ice monolayer" in contrast to multilayer CI films). The distance between equivalent water molecules along the Mo{−110} direction is 4.45 Å, which is only 1% shorter than that on the ice $I_h$(0001) surface (=4.5 Å). Along the {−1−11} direction, the water−water distance projected onto the Mo surface is equal to 2.73 Å, which is longer than 2.61 Å in the ice bulk. Therefore, the ice lattice must be slightly expanded along the Mo{−1−11} direction. Alternatively, the top water layer can be relaxed inward, thus decreasing the interlayer distance between the water layers. In the absence of the silica film, the ice overlayer would show a (3 × 1) superstructure with respect to the Mo substrate. Since the silica monolayer forms a $c$(2 × 2) structure with respect to Mo(112)-(1 × 1), the ice layer exhibits a $c$(6 × 2) structure when referenced to Mo(112) and a $c$(2 × 2) structure with respect to the silica surface.

Assuming that the substrate phonon shift is caused by the polarization of the Si−O−Mo bond, small variations in the interface structure will manifest itself through the extent of the phonon shift, which is the smallest for the amorphous layer. The effect is expected to be the strongest for the ice monolayer, which is in a good epitaxial relationship with the substrate. Additional water adsorption destroys the ordered structure as observed by LEED, probably due to the growth of 3D crystallites on top of the ice monolayer. In addition, the next layers may also change the net dipole moment of the ice normal to the surface, which is shown to be thickness-dependent.[60,61] Both these effects will diminish the extent of the phonon shift. Therefore, the observed shift will be smaller (larger) with increasing (decreasing) the film thickness as observed in Figure 3.

Based on the IRAS spectra, showing a signal from the bare silica, in particular at low coverages where the ice monolayer structures are presumably formed, these films are not dense and expose silica substrate. For example, the film may consist of monolayer islands covering the substrate. Alternatively, the film may expose nanopatterned structures as observed by STM on Pd(111)[22] or well-oriented stripes as observed on the Cu(110) surface.[23] Further STM and AFM studies of these systems in combination with theoretical calculations would help in understanding the structure of the ice overlayers on the well-ordered silica films.

## 5. Summary

We have studied low-temperature adsorption of water on a thin silica film grown on Mo(112) by TPD, IRAS, and PES. Adsorption at 100 K exhibits a zero-order desorption kinetics and increases the phonon frequency of the silica film (at 1059 $cm^{-1}$) by 9 $cm^{-1}$ at most. In contrast, TPD spectra of water adsorbed at 140 K to the same water coverage are shifted to higher temperatures (by ∼7 K at one monolayer) and show a pseudo-first-order desorption kinetics. The "high-temperature" adsorption results in an IRAS signal blue-shifted by ∼20 $cm^{-1}$. Even larger spectral shifts are observed for the $D_2O$ adsorption. The results were rationalized in terms of the formation of amorphous solid water film at 100 K and an ice monolayer film at 140−150 K. This layer is well-ordered as revealed by LEED, showing a $c$(2 × 2) superstructure with respect to the silica substrate.

**Acknowledgment.** The support from the Fonds der Chemischcn Industrie and the EU project GSOMEN is gratefully acknowledged. J.W. and D.S. thank Alexander von Humboldt Foundation for a fellowship. S.K. thanks International Max-Planck Research School "Complex surfaces in materials science" for a fellowship. We also acknowledge Junling Lu and Helmut Kuhlenbeck for the technical assistance and Dietrich Menzel for fruitful discussions.

## References and Notes

(1) Thiel, P. A.; Madey, T. E. *Surf. Sci. Rep.* **1987**, *7*, 211.
(2) Henderson, M. A. *Surf. Sci. Rep.* **2002**, *46*, 5.
(3) Haq, S.; Harnett, J.; Hodgson, A. *Surf. Sci.* **2002**, *505*, 171.
(4) Ogasawara, H.; Brena, B.; Nordlund, D.; Nyberg, M.; Pelmenschikov, A.; Pettersson, L. G. M.; Nilsson, A. *Phys. Rev. Lett.* **2002**, *89*, 276102.
(5) Morgenstern, M.; Michely, T.; Comsa, G. *Phys. Rev. Lett.* **1996**, *77*, 703.
(6) Clay, C.; Haq, S.; Hodgson, A. *Phys. Rev. Lett.* **2004**, *92*, 046102.
(7) Mitsui, T.; Rose, M. K.; Fomin, E.; Ogletree, D. F.; Salmeron, M. *Science* **2002**, *297*, 1850.
(8) Held, G.; Menzel, D. *Phys. Rev. Lett.* **1995**, *74*, 4221.
(9) Feibelman, P. J. *Science* **2002**, *295*, 99.
(10) Weissenrieder, J.; Mikkelsen, A.; Andersen, J. N.; Feibelman, P. J.; Held, G. *Phys. Rev. Lett.* **2004**, *93*, 196102.
(11) Andersson, S.; Nyberg, C.; Tengstal, C. G. *Chem. Phys. Lett.* **1984**, *104*, 305.
(12) Yamamoto, S.; Beniya, A.; Mukai, K.; Yamashita, Y.; Yoshinobu, J. *J. Phys. Chem. B* **2005**, *109*, 5816.
(13) Doering, D. L.; Madey, T. E. *Surf. Sci.* **1982**, *123*, 305.
(14) Held, G.; Menzel, D. *Surf. Sci.* **1994**, *316*, 92.
(15) Glebov, A.; Graham, A. P.; Menzel, A.; Toennies, J. P. *J. Chem. Phys.* **1997**, *106*, 9382.
(16) Kretzschmar, K.; Sass, J. K.; Bradshaw, A. M; Holloway, S. *Surf. Sci.* **1982**, *115*, 183.
(17) Michaelides, A.; Alavi, A.; King, D. A. *Phys. Rev. B* **2004**, *69*, 113404.
(18) Kimmel, G. A.; Petrik, N. G.; Dohnalek, Z.; Kay, B. D. *Phys. Rev. Lett.* **2005**, *95*, 166102.
(19) Morgenstern, M.; Muller, J.; Michely, T.; Comsa, G. *Z. Phys. Chem.-Int. J. Res. Phys. Chem. Chem. Phys.* **1997**, *198*, 43.
(20) Morgenstern, K.; Rieder, K. H. *J. Chem. Phys.* **2002**, *116*, 5746.
(21) Morgenstern, K.; Nieminen, J. *Phys. Rev. Lett.* **2002**, *88*, 066102.
(22) Cerda, J.; Michaelides, A.; Bocquet, M. L.; Feibelman, P. J.; Mitsui, T.; Rose, M.; Fomin, E.; Salmeron, M. *Phys. Rev. Lett.* **2004**, *93*, 116101.
(23) Yamada, T.; Tamamori, S.; Okuyama, H.; Aruga, T. *Phys. Rev. Lett.* **2006**, *96*, 036105.
(24) Stirniman, M. J.; Huang, C.; Smith, R. S.; Joyce, S. A.; Kay, B. D. *J. Chem. Phys*. **1996**, *105*, 1295.
(25) Leist, U.; Ranke, W.; Al-Shamery, K. *Phys. Chem. Chem. Phys.* **2003**, *5*, 2435.
(26) Yang, J. J.; Wang, E. G. *Phys. Rev. B* **2006**, *73*, 035406.
(27) Abu Haija, M.; Guimond, S.; Uhl, A.; Kuhlenbeck, H.; Freund, H. J. *Surf. Sci.* **2006**, *600*, 1040.
(28) Heidberg, J.; Redlich, B.; Wetter, D. *Ber. Bunsen-Ges. Phys. Chem. Chem. Phys.* **1995**, *99*, 1333.
(29) Xu, C.; Goodman, D. W. *Chem. Phys. Lett.* **1997**, *265*, 341.
(30) Ferry, D.; Glebov, A.; Senz, V.; Suzanne, J.; Toennies, J. P.; Weiss, H. *J. Chem. Phys.* **1996**, *105*, 1697.
(31) Ferry, D.; Picaud, S.; Hoang, P. N. M.; Girardet, C.; Giordano, L.; Demirdjian, B.; Suzanne, J. *Surf. Sci.* **1998**, *409*, 101.
(32) Giordano, L.; Goniakowski, J.; Suzanne, J. *Phys. Rev. Lett.* **1998**, *81*, 1271.
(33) Wang, Y.; Truong, T. N. *J. Phys. Chem. B* **2004**, *108*, 3289.
(34) Tzvetkov, G.; Zubavichus, Y.; Koller, G.; Schmidt, T.; Heske, C.; Umbach, E.; Grunze, M.; Ramsey, M. G.; Netzer, F. P. *Surf. Sci.* **2003**, *543*, 131.
(35) Joseph, Y.; Ranke, W.; Weiss, W. *J. Phys. Chem. B* **2000**, *104*, 3224.
(36) Daschbach, J. L.; Dohnalek, Z.; Liu, S. R.; Smith, R. S.; Kay, B. D. *J. Phys. Chem. B* **2005**, *109*, 10362.
(37) Meyer, R.; Baumer, M.; Shaikhutdinov, S. K.; Freund, H.-J. *Surf. Sci.* **2003**, *546*, L813.
(38) Weissenrieder, J.; Kaya, S.; Lu, J. L.; Gao, H. J.; Shaikhutdinov, S.; Freund, H. J.; Sierka, M.; Todorova, T. K.; Sauer, J. *Phys. Rev. Lett.* **2005**, *95*, 076103.
(39) Todorova, T. K.; Sierka, M.; Sauer, J.; Kaya, S.; Weissenrieder, J.; Lu, J. L.; Gao, H. J.; Shaikhutdinov, S.; Freund, H. J. *Phys. Rev. B* **2006**, *73*, 165414.
(40) Wendt, S.; Frerichs, M.; Wei, T.; Chen, M. S.; Kempter, V.; Goodman, D. W. *Surf. Sci.* **2004**, *565*, 107.
(41) Ogasawara, H.; Yoshinobu, J.; Kawai, M. *Chem. Phys. Lett.* **1994**, *231*, 188.
(42) Smith, R. S.; Huang, C.; Wong, E. K. L.; Kay, B. D. *Surf. Sci.* **1996**, *367*, L13.
(43) Clay, C.; Haq, S.; Hodgson, A. *Chem. Phys. Lett.* **2004**, *388*, 89.
(44) Ozensoy, E.; Szanyi, J.; Peden, C. H. F. *J. Phys. Chem. B* **2005**, *109*, 3431.
(45) Chakarov, D. V.; Osterlund, L.; Kasemo, B. *Vacuum* **1995**, *46*, 1109.
(46) Speedy, R. J.; Debenedetti, P. G.; Smith, R. S.; Huang, C.; Kay, B. D. *J. Chem. Phys.* **1996**, *105*, 240.
(47) Haynes, D. R.; Tro, N. J.; George, S. M. *J. Phys. Chem.* **1992**, *96*, 8502.
(48) Whalley, E. *Can. J. Chem.-Rev. Can. Chim.* **1977**, *55*, 3429.
(49) Buch, V.; Devlin, J. P. *J. Chem. Phys.* **1999**, *110*, 3437.
(50) Horn, A. B.; Chesters, M. A.; McCoustra, M. R. S.; Sodeau, J. R. *J. Chem. Soc.-Faraday Trans.* **1992**, *88*, 1077.
(51) Mate, B.; Medialdea, A.; Moreno, M. A.; Escribano, R.; Herrero, V. J. *J. Phys. Chem. B* **2003**, *107*, 11098.
(52) Callen, B. W.; Griffiths, K.; Norton, P. R. *Surf. Sci.* **1992**, *261*, L44.
(53) Rowland, B.; Fisher, M.; Devlin, J. P. *J. Chem. Phys.* **1991**, *95*, 1378.
(54) Cappus, D.; Xu, C.; Ehrlich, D.; Dillmann, B.; Ventrice, C. A.; Alshamery, K.; Kuhlenbeck, H.; Freund, H. J. *Chem. Phys.* **1993**, *177*, 533.
(55) Lemire, C.; Meyer, R.; Henrich, V. E.; Shaikhutdinov, S.; Freund, H. J. *Surf. Sci.* **2004**, *572*, 103.
(56) Yamada, T.; Okuyama, H.; Aruga, T.; Nishijima, M. *J. Phys. Chem. B* **2003**, *107*, 13962.
(57) Frank, M.; Wolter, K.; Magg, N.; Heemeier, M.; Kuhnemuth, R.; Baumer, M.; Freund, H. J. *Surf. Sci.* **2001**, *492*, 270.
(58) Magg, N.; Immaraporn, B.; Giorgi, J. B.; Schroeder, T.; Baumer, M.; Dobler, J.; Wu, Z. L.; Kondratenko, E.; Cherian, M.; Baerns, M.; Stair, P. C.; Sauer, J.; Freund, H. J. *J. Catal.* **2004**, *226*, 88.
(59) Lu, J. L.; Kaya, S.; Weissenrieder, J.; Gao, H. J.; Shaikhutdinov, S.; Freund, H. J. *Surf. Sci.* **2006**, *600*, L153.
(60) Su, X. C.; Lianos, L.; Shen, Y. R.; Somorjai, G. A. *Phys. Rev. Lett.* **1998**, *80*, 1533.
(61) Witek, H.; Buch, V. *J. Chem. Phys*. **1999**, *110*, 3168.